Environ. Sci. Technol. **2001**, *35,* 2136−2140

Indoor Dose Conversion Coefficients for Radon Progeny for Different Ambient Environments

K. N. YU,*,† B. T. Y. WONG,† J. Y. P. LAW,† B. M. F. LAU,† AND D. NIKEZIC†,‡

Department of Physics and Materials Science, City University of Hong Kong, Tat Chee Avenue, Kowloon Tong, Kowloon, Hong Kong, and Faculty of Sciences, University of Kragujevac, 34000 Kragujevac, Yugoslavia

Inhaled progeny of ^{222}Rn (radon progeny) are the most important source of irradiation of the human respiratory tract. Their attachment to atmospheric aerosols follows a well-established relationship between the activity size distribution (ASD) and the number size distribution. Recent studies have shown that indoor aerosols are derived primarily from outdoor sources, so it is pertinent to study the effects of different ambient environments on the indoor radon dose (in terms of the dose conversion coefficient or DCC, in units of mSv WLM^{-1}). Commonly encountered ambient aerosols were studied here, which included the traffic-, urban-, and marine-influenced aerosols. The ASDs of attached radon progeny for all three studied ambient environments were well-represented by normal distributions. From these ASDs, the DCCs were calculated using the ICRP66 model and the scaled Yeh−Schum model. All other employed parameters were adopted from original references or authoritative reports. The DCCs for a nominal home calculated using the James model and the Yeh−Schum model were 12 and 8 mSv WLM^{-1}, respectively. The DCCs were largest for urban-influenced ambient environments and smallest for marine-influenced ambient environments, and those for traffic-influenced ambient environments were close to that for a nominal home. If we adopt the stochastic model, the probability of contracting radon-induced lung cancer by a person living with a marine-influenced ambient environment will be half that of a person living with an urban-influenced ambient environment.

Introduction

Inhaled progeny of ^{222}Rn (hereafter referred to as radon progeny) are the most important source of irradiation of the human respiratory tract. Epidemiological studies of underground miners of uranium and other minerals have provided reasonably firm estimates of the risk of lung cancer associated with exposure to radon progeny (*1*, *2*). More recently, Lubin et al. (*3*), to provide quantitative information on the risk of radon-induced lung cancer, have carried out a joint analysis of data from 11 studies in which 2700 lung cancer deaths occurred among 68 000 miners, accumulating nearly 1.2 million person-years. Excess relative risk (ERR) of lung cancer was linearly related to cumulative exposure (J/m^3) (or in WLM = 12.6 J/m^3) to radon progeny. The dose conversion coefficient (DCC) obtained from miners' epidemiological studies is about 5 mSv WLM^{-1}. The Scientific Panel appointed by the National Research Council (NRC) has reviewed the basic information and the modeling procedures needed to extend these data to radon exposure in the home environment. The reviews carried out by the NRC's panel and the ICRP Task Group (*4*) both concluded that the target tissue at risk are basal and secretory cells in the epithelium. In the opinion of the NRC, the DCC to characterize the lifetime exposure to radon progeny in homes should be 12 mSv WLM^{-1}. ICRP66 found that it should be 15 mSv WLM^{-1} (*5*). James (*6*) also concluded that the effective dose calculated for exposure to radon progeny needs to be substantially modified to allow dosimetric estimates of lung cancer risk to reconcile with values obtained from epidemiological studies.

In the assessment of health effects due to inhalation of radon progeny aerosols, particle size is one of the most influential parameters (e.g., refs *5* and *7*). The current understanding of properties of indoor radon progeny largely follow the report of the National Research Council (*8*) and references therein, although some modifications and fine-tunings have been adopted by different workers in the field (e.g., see ref *9*). It is generally assumed that the radon dose is contributed by two modes, viz., the unattached mode and the attached mode, governed by the log-normal distribution. The unattached mode has an activity median diameter (AMD) of 1.1 nm with a geometric standard deviation (GSD) of 1.5 (see, for example, ref *5*). The attached mode for a typical indoor environment has an AMD of 200 nm, while that for an indoor environment with the presence of cigarette smoke as well as that for mine atmospheres has an AMD of 250 nm. The GSD is calculated by the expression given by International Commission on Radiological Protection (*10*) as

$$\mathrm{GSD} = 1 + 1.5\{1 - [100(\mathrm{AMD}\ (\mu\mathrm{m}))^{1.5} + 1]^{-1}\} \quad (1)$$

Castleman (*11*) suggested that the unattached radon progeny contains between 5 and 8 water molecules. Although there are some arguments against the log-normal behavior of the unattached radon progeny based on the suggestion of Castleman (*11*), the log-normal behavior has been generally accepted in the field of radon research (e.g., refs *5*, *8*, *10*, and *12*−*15*). If other types of distribution can be found in the future that better fit the behavior of unattached radon progeny, the formulations in the present paper can be easily modified to accommodate such changes.

Processes exist in an indoor environment (cleaning using a vacuum cleaner, cooking, using home heating systems, etc.) that can produce an additional mode (called the nucleation mode) with an AMD of around 20 nm. For other activities such as cleaning using a vacuum cleaner and cooking, the nucleation mode is transient with a lifetime of only a few hours. Tu et al. (*7*) conducted size distribution measurements of radon progeny particles in a variety of indoor environments in urban, suburban, and rural areas. They found that the radon progeny particle size distribution due to indoor activities has two definable source categories: (i) gas combustion from stoves and kerosene heaters and (ii) cigarette smoking and food frying. Although efforts have been spent on investigating the effects of different indoor activities on the indoor radon dose, the effects of different (outdoor) ambient environments on the indoor radon dose have not been extensively studied.

* Corresponding author e-mail: peter.yu@cityu.edu.hk; phone: (852)27887812; fax: (852)27887830.
† City University of Hong Kong.
‡ University of Kragujevac.

10.1021/es001920k CCC: $20.00

Published on Web 04/25/2001

There have been investigations that studied the contribution of outdoor particle sources to indoor concentrations. For example, Abt et al. (*16*) showed that outdoor particles (20−500 nm) contributed significantly to indoor particle levels. Effective penetration efficiencies ranged from 0.38 to 0.94 for 20−500-nm particles. These estimates were in the range of values of Koutrakis and Briggs (*17*) and Suh et al. (*18*). Suh et al. (*18*) reported effective penetration efficiencies of 0.36 for air-conditioned homes (median air exchange rate $\approx 0.3\ h^{-1}$) and 0.78 for nonair-conditioned homes (median air exchange rate $\approx 2\ h^{-1}$), while Koutrakis and Briggs (*17*) estimated a value of 0.49 for sulfate and $PM_{2.5}$. Abt et al. (*16*) also concluded that, for 20−300-nm particles, 63−92% of indoor concentrations are from outdoor sources while 8−37% are from indoor sources, i.e., these particles are derived primarily from outdoor sources. Tong and Lam (*19*) also showed that traffic is an important factor in affecting the household dust contamination in high-rise buildings in Hong Kong. Therefore, it is pertinent to study the effects of different ambient environments on the indoor radon dose (in terms of the DCC).

Size Distribution of Aerosols

Number Size Distribution. Knowledge of the distribution of outdoor airborne particulate matter into size fractions has become an increasing area of focus when examining the effects of air pollution since they are important for exposure and risk assessment. However, the limited number of works devoted to investigations of modality in outdoor particle size distributions makes it difficult to conduct more comprehensive comparisons and to draw global conclusions on the topic (*20*).

Recently, Morawska et al. (*20*) conducted a systematic analysis of over 6000 size distribution spectra collected over a period of 3 yr, for a range of different ambient conditions including traffic-influenced, urban, vegetation burning, marine, modified background, and suburban. The size range covered 16−30 000 nm through using a scanning mobility particle sizer and an aerodynamic particle sizer for various ambient aerosols. The commonly encountered ambient aerosols will be employed for the present study, which include the traffic-, urban-, and marine-influenced aerosols.

The number size distribution (NSD) for the freeway-influenced aerosols presented by Morawska et al. (*20*) had two prominent modes at about 20−40 and 1000−2000 nm in the NSD. These spectra were very similar to those measured for gasoline exhaust particle size distribution (*21*), and it was thus considered reasonable to conclude that gasoline exhaust is the major aerosol source for their NSD. The two modes identified were similar to those found in the literature (*22*−*24*).

The NSD for the urban-influenced aerosols presented by Morawska et al. (*20*) contained two predominant modes in the 20−40- and 800−900-nm particle size ranges. The nuclei mode (at 20−40 nm) compared favorably to the location of the same mode for the traffic-influenced aerosols, although the peak was not as well-defined for the urban-influenced aerosol.

There were a number of peaks present within the modes of the marine-influenced aerosol NSD presented by Morawska et al. (*20*). The nuclei mode at approximately 40 nm was consistent with a marine-influenced or free troposphere nuclei mode.

Activity Size Distribution. The radon progeny will attach to atmospheric aerosols. The activity size distribution $C(\mathrm{d})$ and the number size distribution $Z(\mathrm{d})$ of the aerosols are different because the attachment probability $\beta(\mathrm{d})$ is a function of particle diameter d (e.g., ref *12*). The relationship between both size distributions is given by (*12*)

$$C(\mathrm{d}) = [C/X]\,\beta(\mathrm{d})\,Z(\mathrm{d}) \qquad (2)$$

where C is the radionuclide concentrations, X is the attachment rate expressing the adsorption velocity of the radon progeny to the aerosol with the number concentration Z and the attachment coefficient $\beta(\mathrm{d})$ described by

$$\beta(\mathrm{d}) = \frac{2\pi D_c d}{\dfrac{8D_c}{\mathrm{d}\bar{\nu}} + \dfrac{d}{d + l_c}} \qquad (3)$$

where $D_c = 6.8 \times 10^{-2}\ cm^2\ s^{-1}$ is the mean diffusion coefficient, $\bar{\nu} = 1.7 \times 10^4\ cm\ s^{-1}$ is the mean thermal velocity, and $l_c = 4.9 \times 10^{-6}$ cm is the mean free path of the radon progeny.

The final DCCs (in $mSv\ WLM^{-1}$) are going to be calculated for a home (with different ambient environments), i.e., the unattached fraction of the potential α energy concentration (PAEC) = 0.08; activity median diameter of unattached radon progeny $AMD_u = 1.1$ nm. As mentioned before, the indoor aerosols are derived primarily from outdoor sources, so we assume that the indoor NSD can be sufficiently represented by the corresponding (outdoor) NSD of the ambient environment. From the NSD, the activity size distribution for attached radon progeny can be depicted, and from which the parameters can be obtained by least-squares fitting.

It is interesting to find that the activity size distributions of attached radon progeny for all three studied ambient environments are well-represented by normal distributions, although there is a second minor log-normal peak for the marine-influenced ambient environments (accounting for only about 2.5% of the total PAEC). While log-normal distributions are characterized by the AMD and the GSD, normal distributions are characterized by the mean and the standard deviation (SD).

DCC values are also calculated for a nominal home environment for reference, i.e., the unattached fraction of PAEC = 0.08; activity median diameter of unattached radon progeny $AMD_u = 200$ nm; and GSD is calculated by eq 1 as 2.35. The parameters of the activity size distribution for attached radon progeny for traffic-, urban-, and marine-influenced ambient environments and those for the nominal home environment are listed in Table 1.

TABLE 1. Parameters of Activity Size Distribution for Attached Radon Progeny for Traffic-, Urban-, and Marine-Influenced Ambient Environments and for a Typical Home Environment

	AMD (nm)	GSD	mean (nm)	SD (nm)
traffic			223	136
urban			135	69
marine	338	1.4	70	18
nominal home	200	2.35		

Dosimetric Lung Models

Calculation of the dose delivered by radon progeny to the tracheobronchial (T-B) tree requires many models such as the deposition model, clearance model, dose calculation model, and morphometry model of the T-B tree.

The morphometry models used in the present work are the ICRP66 symmetrical model (*10*) and the Yeh−Schum asymmetrical model (*25*). James (*26*) has calculated the means of the airway dimensions from the models of Weibel (*27*), Yeh and Schum, and Phalen et al. (*28*), known as the UCI model. The NRC panel has used one version of this model. Yeh and Schum (*25*) have made extensive measurements of the airways, which are also currently used. James (*29*) proposed a way to scale down a model according to the lung

TABLE 2. Dimensions for Yeh−Schum Asymmetrical Model[a]

	right lobes						left lobes			
	upper		middle		lower		upper		lower	
generation	*L*	*D*	*L*	*D*	*L*	*D*	*L*	*D*	*L*	*D*
0	10.0	2.01	10.0	2.01	10.0	2.01	10.0	2.01	10.0	2.01
1	3.09	1.75	3.09	1.75	3.09	1.75	5.63	1.38	5.63	1.38
2	1.22	1.02	3.02	1.33	3.02	1.33	1.45	1.03	1.42	1.15
3	0.800	0.760	2.27	0.720	0.880	1.01	1.08	0.835	1.33	0.905
4	1.27	0.650	1.34	0.620	1.09	0.800	1.02	0.640	1.13	0.680
5	1.25	0.579	1.63	0.528	1.33	0.650	1.09	0.533	0.891	0.559
6	0.827	0.454	1.04	0.376	1.22	0.583	1.02	0.426	1.02	0.454
7	0.988	0.355	1.04	0.317	0.796	0.471	0.751	0.341	0.836	0.365
8	0.798	0.278	0.691	0.268	0.803	0.367	0.832	0.307	0.778	0.316
9	0.557	0.216	0.527	0.199	0.880	0.347	0.555	0.234	0.771	0.298
10	0.401	0.158	0.394	0.147	0.900	0.317	0.482	0.178	0.611	0.286
11	0.350	0.118	0.266	0.106	0.591	0.249	0.388	0.135	0.544	0.211
12	0.250	0.088	0.225	0.083	0.449	0.181	0.343	0.100	0.431	0.146
13	0.194	0.070	0.172	0.064	0.337	0.134	0.267	0.078	0.302	0.102
14	0.143	0.058	0.118	0.051	0.257	0.101	0.215	0.061	0.224	0.076
15	0.113	0.046	0.092	0.040	0.222	0.077	0.169	0.048	0.188	0.061
16	0.088	0.036	0.074	0.032	0.158	0.066	0.134	0.038	0.148	0.048

[a] *L*, length; *D*, diameter; both in centimeters.

TABLE 3. Dimensions (cm) for the ICRP66 Symmetrical Model

	diameter	length		diameter	length		diameter	length
0	1.65	9.1	6	0.29	0.66	12	0.088	0.25
1	1.2	3.8	7	0.24	0.60	13	0.072	0.20
2	0.85	1.5	8	0.2	0.53	14	0.060	0.17
3	0.61	0.83	9	0.16	0.44	15	0.053	0.14
4	0.44	0.9	10	0.13	0.36	16	0.042	0.1087
5	0.36	0.81	11	0.11	0.30			

volume, since the Yeh−Schum model had a much larger volume than other models. The dimension of airway tubes of the two models are listed in Tables 2 and 3.

The DCCs were calculated using programs developed by us. A flowchart of the programs used is given in Figure 1. As can be seen from Figure 1, the calculations of DCCs involved two phases and made use of two separate programs, namely, CCOEF and LUNG.

The first computer program, CCOEF, calculated the absorbed dose per unit surface activity on the inner bronchi wall. In this work, our attention is confined to the calculation of dose to the basal and secretory cells in the epithelium due to 6 MeV α-particles from ^{218}Po and 7.69 MeV α-particles from ^{214}Po, the ranges of which are taken to be 48 and 71 μm, respectively, in tissue (tissue-equivalent liquid). Stopping powers for α-particles in striated muscle (*30*) have been employed.

In the present work, the idealized picture of the epithelium used is as illustrated by the NRC panel (*8*), i.e., the airway consists of cylindrical tubes. In the bronchial (BB) region (generations 1−8), the tubes have a 5-μm layer of mucous gel and a 6-μm layer of cilia and fluid, and the basal and secretory cells are distributed between 35 and 50 μm and between 10 and 40 μm, respectively, below the epithelial surface. In the bronchiolar (bb) region (generations after 8), the tubes have a 2-μm layer of mucous gel and a 4-μm layer of cilia and fluid, and there are no basal cells; the secretory cells are distributed between 4 and 12 μm below the epithelial surface. As earlier, the calculation takes into account the dose contributed by α-particles crossing the airway lumen (the so-called far wall contribution).

Radon progeny were taken to be homogeneously distributed in the mucous layer. The emission of the α-particle from a point in the mucous layer, i.e., its starting point as well as its direction, have been sampled by a Monte Carlo method. The next step is to calculate the distances the α-particle has traveled in tissue from its point of origin to the entrance/exit points in the basal and secretory layers, from which energy loss in the basal or secretory layer has been calculated.

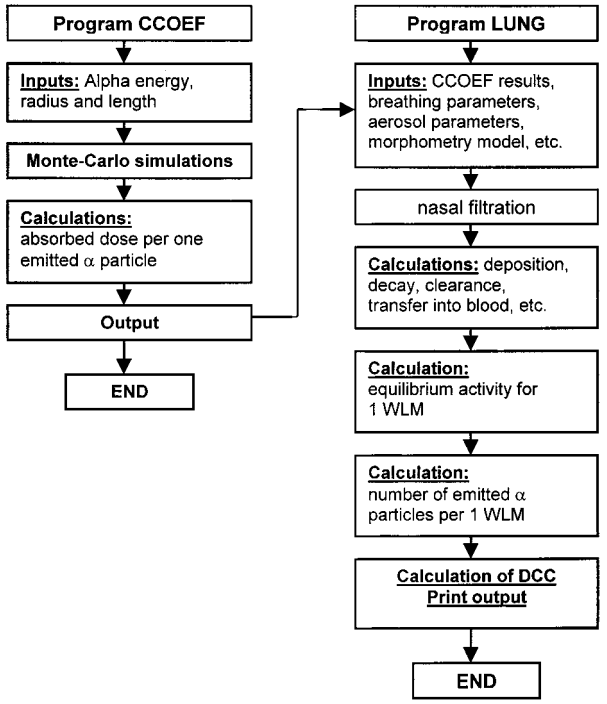

FIGURE 1. Flowchart of the programs used to calculate the dose conversion coefficients (DCCs), which involve two phases and two separate programs, namely, CCOEF and LUNG.

The amount of energy deposited in the target cells depended on the stopping power of the α-particles in the tissue. The experimental information about slowing down of α-particles in tissue was given in ICRU49 (*30*). The data given by ICRU49 were fitted by the seventh-order polynomial in the low energy region below 2 MeV:

$$-\frac{dE}{dx} = c_1 + c_2E + c_3E^2 + c_4E^3 + c_5E^4 + c_6E^5 + c_7E^6 + c_8E^7 \quad (4)$$

where $c_1 = 332.201$, $c_2 = 11465.956$, $c_3 = -34405.805$, $c_4 = 65160.750$, $c_5 = -74817.644$, $c_6 = 48668.099$, $c_7 = -16413.770$, and $c_8 = -2225.653$ (*31*). In the higher energy region (above 2 MeV), another sixth-order polynomial fit was used with the parameters as $c_1 = 3457.934$, $c_2 = -1577.94579$, $c_3 = 459.64431$, $c_4 = -81.19981$, $c_5 = 8.44979$, $c_6 = -0.47563$, and $c_7 = 0.01115$ (*31*). Therefore, eq 4 with two sets of the parameters was employed to determine the absorbed doses per unit exposure to radon progeny in sensitive cells of the bronchial epithelium.

In this method, the above steps for the Monte Carlo simulation have been repeated 10^4 times. The average absorbed dose in the interested layers (basal and secretory cells) have then been calculated for one α-particle by dividing the average energy with the mass of the basal or secretory layer. This quantity, called the conversion coefficient (CC), was given in units of MeV per α-particle. Using the inner surface area of the airway, this figure can then be converted into absorbed dose per unit surface activity. This concludes our first program, CCOEF.

The results obtained in the first phase of calculation were used in the second program, LUNG. In our model, each airway tube in the various generations was treated separately. The main objective in the second phase was to obtain the equilibrium activity and the number of emitted α-particles (N_α) of radon progeny in every airway tube for the exposure of 1 WLM. The equilibrium activity is the activity of some radon progeny in an airway in generation *j*, which is established as the balance between the processes that increase its activity (deposition + decay of the parent nuclide in the radioactive chain + activity cleaned and transported by mucus from generations $>j$) and those processes that decrease its activity (decay, transfer to blood, cleaned and transported by mucus into generations $<j$). N_α was found in the present paper as the number of α-particles per WLM. The product of $N_\alpha \times$ CC gave the DCF (in mGy WLM^{-1}) for the sensitive cells.

As the first step, the nasal filtration of the aerosol particles and the unattached fraction have been estimated using the work of Cheng et al. (*32*). The deposition in the airways has been considered both for inspiration and expiration. The deposition equation of Cohen and Asgharian (*33*), applicable in the region 0.04−0.2 μm, has been used together with Gormley and Kennedy expressions (*34*) with Landahl corrections (*35*). For the calculation of diffusion coefficients of aerosol particles, the NRC panel treatment has been followed. To calculate the equilibrium activity, the mucous transit time, as given by Cuddihy and Yeh (*36*), quoted also by NRC, was used. Two main clearance routes were considered: mucus clearance and transfer to blood. The transfer into the blood was characterized by the half-time of $T = 600$ min (*8*), and the mucous clearance rate throughout the T-B tree was also taken from the NRC (*8*).

The DCCs were finally obtained by multiplying the number of α-particles emitted by ^{218}Po and ^{214}Po for the exposure of 1 WLM with the corresponding conversion coefficients. After obtaining the DCCs in different generations of the T-B tree, an average one was calculated by weighting them with the surface area in the corresponding generation. This concludes our second program, LUNG.

It is noted here that all the parameters employed in the above computations were adopted from original references or authoritative reports such as those of the NRC and the ICRP, e.g., depths and layer thickness of mucous gel, cilia and fluid, and the basal and secretory cells, breathing rates, respiratory frequencies, mucous transit time for different generations, transfer half-time into the blood, mucous clearance rate throughout the T-B tree, etc. Sensitivity analysis of these adopted parameters can be found in refs *5* and *37*).

The final DCCs (in mSv WLM^{-1}) are calculated for different homes (with different ambient environments) as described in the previous section. The radiation weighting factor for α-radiation $w_R = 20$ was used. Tissue weighting factors $w = 0.5$ for basal and secretory cells in BB region were adopted. The dose in secretory and basal cells were multiplied by 0.5 and summed up. The tissue weighting factor in the bb region where secretory cells are the only sensitive cells was taken as 1. The total dose was then evaluated as the sum of the doses in the BB and bb regions that had been multiplied with 0.333 (as recommended by ICRP66), which was then multiplied by the tissue weighting factor $w_t = 0.12$ for lung to get the effective dose.

TABLE 4. Dose Conversion Coefficients (mSv WLM^{-1}) for Traffic-, Urban-, and Marine-Influenced Ambient Environments

	James model	Yeh−Schum model
traffic	11.9	7.9
urban	15.2	10.9
marine	8.4	4.8
nominal home	12.0	8.1

Results and Discussion

The DCCs for traffic-, urban-, and marine-influenced ambient environments obtained using the James model and the Yeh−Schum model are listed in Table 4. The DCC for a nominal home calculated using the James model is 12 mSv WLM^{-1}, which is the same as that given by the NRC and close to the ICRP66 value of 15 mSv WLM^{-1} (*5*). The corresponding value obtained using the Yeh−Schum model is 8 mSv WLM^{-1}. It is also observed that the ICRP66 model consistently gave larger DCCs than the Yeh−Schum model, which was explained by the difference in their total surface areas of the T-B tree (*31*). As mentioned before, the effective dose calculated for exposure to radon progeny needs to be scaled to compare with values obtained from epidemiological studies (*6*). Therefore, the pattern of variation is more important than the absolute values. It can be seen in Table 4 that both models presented the same pattern of variation in the DCC values.

It can be observed that the DCCs are largest for urban-influenced ambient environments and smallest for marine-influenced ambient environments, and those for traffic-influenced ambient environments are close to that for a nominal home. The trend is somewhat expected if we think in terms of the corresponding aerosol sizes. Apparently, the large-aerosol fraction decrease from urban-influenced ambient environments to traffic-influenced ambient environments and then to marine-influenced ambient environments. Diffusion deposition, which is an efficient mechanism for radon progeny deposition in the tracheobronchial tree, operates essentially only for small particles (unattached mode and the nucleation mode). For larger particles, non-diffusion deposition is more effective, and the calculated DCCs are thus smaller for lower large-aerosol fractions.

In conclusion, the DCC can be halved when one lives in an area when the marine-influenced aerosols predominate, e.g., near the sea and away from the urban area. If we adopt the widely accepted stochastic model for radon-induced lung cancers, given the same building characteristics and the same exposure to radon progeny, the probability of contracting radon-induced lung cancer by a person living with a marine-influenced ambient environment will also be half that of a person living with an urban-influenced ambient environment.

Acknowledgments

This research is supported by CERG Grant CityU1004/99P from the Research Grant Council of Hong Kong.

Literature Cited

(1) Lubin, J. H. *Yale J. Biol. Med.* **1988**, *61*, 195.
(2) Muirhead, C. R. In *Radon Measurements by Etched Track Detectors: Applications to Radiation Protection, Earth Sciences and the Environment*; Durrani, S. A., Ilic, R., Eds.; World Scientific: Singapore, 1997; pp 243−257.
(3) Lubin, J. H.; Boyce, J. D.; Edling, C.; Hornung, R. W.; Howe, J.; Kunz, E.; Kusiac, R. A.; Morrison, H. I.; Radford, E. P.; Samet, J. M.; Timarche, M.; Woodward, A.; Xiang, Y. S.; Pierce, D. A. *Radon and Lung Cancer*; U.S. Department of Health and Human Services: Washington, DC, 1994; NIH 94-3644.
(4) Bair, W. J. *Radiat. Prot. Dosim.* **1991**, *38*, 147.
(5) Birchall, A.; James, A. C. *Radiat. Prot. Dosim.* **1994**, *53*, 133.
(6) James, A. C. In *Indoor Radon and Lung Cancer. Reality or Myth*; Cross, F. T., Ed.; Proceedings of 29th Hanford Symposium on Health and Environment; Battelle: Richland, WA, 1992; pp 167−198.
(7) Tu, K. W.; Knutson, E. O.; George, A. C. *Aerosol Sci. Technol.* **1991**, *15*, 170.
(8) National Research Council. *Comparative Dosimetry of Radon in Mines and Homes*; National Academic: Washington, DC, 1991.
(9) Ramamurthi, M.; Hopke, P. K. *Health Phys.* **1989**, *56*, 189.
(10) International Commission on Radiological Protection. *Human Respiratory Tract Model for Radiological Protection*; Pergamon: Oxford, 1994; ICRP Publication 66.
(11) Castleman, A. W., Jr. *Environ. Sci. Technol.* **1991**, *25*, 730.
(12) Porstendörfer, J. *Environ. Int.* **1996**, *22* (Suppl. 1), S563.
(13) Yu, K. N.; Guan, Z. J. *Health Phys.* **1998**, *75*, 147.
(14) Yu, K. N.; Guan, Z. J.; Cheung, T. T. K. *Atmos. Environ.* **1999**, *33*, 4935.
(15) Porstendörfer, J.; Reineking, A. *Health Phys.* **1999**, *76*, 300.
(16) Abt, E.; Suh, H. H.; Catalano, P.; Koutrakis, P. *Environ. Sci. Technol.* **2000**, *34*, 3579.
(17) Koutrakis, P.; Briggs, S. L. K. *Environ. Sci. Technol.* **1992**, *26*, 521.
(18) Suh, H. H.; Koutrakis, P.; Spengler, J. D. *J. Exp. Anal. Environ. Epidemiol.* **1994**, *4*, 1.
(19) Tong, S. T. Y.; Lam, K. C. *Sci. Total Environ.* **2000**, *256*, 115.
(20) Morawska, L.; Thomas, S.; Jamriska, M.; Johnson, G. *Atmos. Environ.* **1999**, *33*, 4401.
(21) Morawska, L.; Thomas, S.; Bofinger, N. D.; Wainwright, D.; Neale, D. *Atmos. Environ.* **1998**, *32*, 2467.
(22) Trier A. *Atmos. Environ.* **1997**, *31*, 909.
(23) Whitby, K. T.; Clark, W. E.; Marple, V. A.; Sverdrup, G. M.; Sem, G. J.; Willeke, K.; Liu, B. Y. H.; Pui, D. Y. H. *Atmos. Environ.* **1975**, *9*, 463.
(24) Li, C. S.; Lin, W. H.; Jenq, F. T. *Atmos. Environ.* **1993**, *27B*, 413.
(25) Yeh, H. C.; Schum, G. M. *Bull. Math. Biol.* **1980**, *42*, 461.
(26) James, A. C. In *Radon and Its Decay Products*; Nazaroff, W., Nero, A., Eds.; Wiley: New York, 1988.
(27) Weibel, E. R. *Morphometry of the Human Lung*; Academic: New York, 1963.
(28) Phalen, R. F.; Oldham, L. J.; Beaucage, C. B.; Crocker, T. T.; Mortensen, J. D. *Anat. Rec.* **1985**, *212*, 368.
(29) James, A. C. *Dosimetry Aspects of Exposure to Radon and Thoron Daughter Product*; Report by a Group of Experts of the OECD Nuclear Energy Agency; 1983.
(30) International Commission on Radiation Units and Measurements (ICRU). *Stopping Powers and Ranges for Protons and Alpha Particles*; ICRU: 1993; ICRU Report 49.
(31) Nikezic, D.; Yu, K. N.; Cheung, T. T. K.; Haque, A. K. M. M.; Vucic, D. *J. Environ. Radioact.* 2000, *47*, 263.
(32) Cheng, Y. S.; Swift, D. L.; Yamada, Y.; Yeh, H. C. *J. Aerosol Sci.* **1988**, *19*, 741.
(33) Cohen, B. S.; Asgharian, B. *J. Aerosol Sci.* **1990**, *21*, 789.
(34) Gormley, P. G.; Kennedy, M. *Proc. R. Irish Acad.* **1949**, *A52*, 163.
(35) Landahl, H. D. *Bull. Math. Biophys.* **1963**, *25*, 29.
(36) Cuddihy, R. G.; Yeh, H. C. In *Inhalation Toxicology: The Design and Interpretation of Inhalation Studies and Their Uses in Risk Assessment*; Mohr, U., Ed.; Springer-Verlag: New York, 1988; pp 169−193.
(37) Marsh, J. W.; Birchall, A. *Radiat. Prot. Dosim.* **2000**, *87*, 167.

Received for review November 30, 2000. Revised manuscript received February 22, 2001. Accepted February 26, 2001.

ES001920K